Experiments in Fluids 15, 147–154 (1993)

Experiments in Fluids

Internal waves generated by the turbulent wake of a sphere

Qiang Lin, D. L. Boyer, H. J. S. Fernando

Department of Mechanical and Aerospace Engineering Tempe, AZ 85287-6106, USA

Received: 18 January 1993 / Accepted: 31 January 1993

Abstract. Internal waves generated by the turbulent wake of a sphere travelling horizontally through a linearly stratified fluid were studied using shadowgraph and particle-streak photography. The Reynolds and internal Froude number ranges considered were 2,000 $\leq$ Re $\leq$ 12,900 and 2.0 $\leq$ Fi $\leq$ 28.0, respectively. Two quite distinct flow regimes based on the structure of the turbulent wake were identified. In one, the wake is characterized by "large-scale coherent structures". In the other, the wake, as viewed on a side-view shadowgraph, grows in a roughly symmetric fashion to a maximum height and then collapses slowly; such flows are termed the "small-scale structures" regime.

Wave lengths and maximum wave heights of the internal waves were measured as functions of Nt and Fi, where N is the Brunt-Väisälä frequency and t the time. It was found that the wave lengths scale well with the streamwise dimension of the spiralling coherent structures. The maximum amplitude of the internal waves were found to scale with the vertical dimension of the turbulent wake, upon varying the internal Froude number.

1 Introduction

Studies of turbulent wakes behind bluff bodies in stratified fluids are of major practical importance in many areas of geophysical sciences and engineering. Some pertinent examples are the wakes of submarines moving through a thermocline (Gilreath and Brandt 1985), air flow past mountains (Brighton 1978; Castro et al. 1983), ocean currents past such natural submarine features as seamounts and man-made underwater structures and the motion of aircraft in the stratosphere. One distinctive feature of stratified turbulent wakes is the coexistence of the turbulence with a field of internal gravity waves excited by the interaction between (i) the body and the stratified fluid (body-generated waves) or (ii) the wake itself and the background stratification (wake-generated waves). In general, the resulting wave fields can be classified as follows:

(i) Lee waves – obstacle generated waves, which are stationary with respect to the body;

(ii) Forced waves – waves generated by time-dependent forcing in the wake due to vortex shedding or turbulence; and

(iii) Waves generated by the gravitational collapse of the turbulent wake – during the physical collapse of the wake, owing to stratification, the potential energy released can appear as internal waves (Wu 1969). Due to the weak mixing that occurs within the wake, however, it is expected that the contribution of this mechanism to the overall gravity wave field is very small.

Theoretical studies of lee wave fields generated by three-dimensional obstacles have been conducted by Crapper (1959) and Lighthill (1978). The phase configuration of internal waves of small amplitude in a density stratified fluid was investigated theoretically, and experimentally by Mowbray and Rarity (1967). Brighton (1978) conducted an experimental investigation of lee waves generated by different obstacles in a water channel. Lin et al. (1992a) delineated the Reynolds (Re) and Froude (Fi) number ranges where lee waves appear for the case of spheres; here $Re = UD/\nu$ and $Fi = U/ND$, where U is the speed of the sphere, D its diameter, ν the kinematic viscosity, $N = (g(d\rho/dz)/\rho_o)^{1/2}$ the buoyancy frequency, $d\rho/dz$ the vertical density gradient of the undisturbed flow and ρ_o a reference density (i.e., at the level of the sphere center). Hopfinger et al. (1991) and Lin et al. (1992a) have measured the wave lengths of lee waves behind spheres, and found good agreement with the predictions of linear theory. Hanazaki (1988) has studied lee wave regimes for a sphere at $Re = 200$ using numerical simulation.

While the various phenomena associated with lee waves have had a fair degree of consideration in the literature, little attention has been given to gravity waves forced by eddy shedding and/or wake turbulence and those caused by gravitational collapse of the wake. Schooley and Hughes (1972) studied the problem of internal waves generated by the collapse of a two-dimensional mixed region in stratified fluids. Gilreath and Brandt (1985) discussed the problem of wave generation

Correspondence to: D. L. Boyer

behind self-propelled bodies. They used ensemble averaged conductivity probe records to study the resulting random field of internal waves (both due to the body and the propeller), and pointed out that linear theory suffered major shortcomings. Chomaz et al. (1990) and Hopfinger et al. (1991) also recently studied the problem of internal waves generated by the body and its wake for spheres moving horizontally through stratified fluids. The latter study visualized internal wave fields using a rake of fluorescein dye lines illuminated by a thin laser sheet for a single $Re = 3{,}000$ and $0.25 \leq Fi \leq 6.25$. It was found that a transition occurs at $Fi \approx 2.0$ from a lee wave regime in the near wake of the sphere to internal gravity waves generated by the coherent turbulent structures in the wake. They did not, however, study the relation between the turbulent wake and the internal wave fields and they did not investigate internal waves generated by the collapse of turbulence in the far wake; i.e., at large $Nt = (X/D)\ Fi^{-1}$, where X is the streamwise coordinate from the sphere center.

The present communication presents quantitative measurements of turbulent wakes and the internal wave fields generated by those wakes for a wide range of Re and Fi. The emphasis is on waves generated by the large coherent structures of the wakes. The measurements on internal wave properties were taken at Reynolds numbers sufficiently large so as to allow the assumption of Re independence on the flow properties. The experimental program considered the parameter ranges $2{,}000 \leq Re \leq 12{,}900$ and $2.0 \leq Fi \leq 28.0$.

2 Experiments

The experiments were conducted in a tow tank 12 m long, 40 cm wide and 30 cm high. Plexiglas spheres of diameter 1.9, 3.17, 3.81 and 5.08 cm, were used for the investigation. Fig. 1 is a schematic diagram of the physical system employed for these experiments. The sphere was mounted on a towing carriage by a thin stainless steel wire passing through its center and connected across two opposite corners of the carriage (see Lin et al. 1992a for details). The speed of the carriage ranged from 10 to 40 cm s^{-1}. While the lower Fi experiments were conducted using the larger spheres, most of the experiments on internal wave fields for higher Fi were performed using the smaller sphere ($D = 1.9$ cm) to reduce the channel confinement effect; i.e., to reduce D/H (the ratio of sphere diameter to fluid depth) and D/W (the ratio of sphere diameter to channel width) to ensure that internal waves are generated with limited interference from surfaces bounding the fluid. Note that the ratio D/H for the current experiments was smaller than that used by Hopfinger et al. (1991), a study which demonstrated, using the large tow tank of the CNRM in France (1 m deep, 3 m wide and 22 m long), that D/H had negligible effect on the wave field.

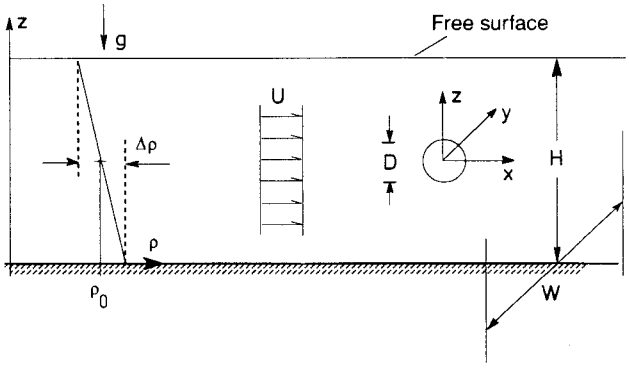

Fig. 1. Physical system

Neutrally buoyant particle tracers were used as the principle technique for visualizing the flow field. In this method, polystyrene particles of nominal diameter 0.05 cm and density 1.040 ± 0.005 g cm^{-3} were used as tracer particles. The natural density variation of the particles and the background density distribution employed were such as to give a relatively uniform particle distribution in the tank. Particle tracer photographs were taken in the vertical streamwise centerplane by illuminating the tracer particles using a plane light sheet approximately 0.5 cm wide. The light source and camera were fixed to the tow-tank in order to remove the large mean velocity. In order to obtain "instantaneous" pictures, the exposure time was kept as short as possible, while in keeping with the detection of the wave fields. The typical exposure time employed was 2 s which is much shorter than the dominant wave period as described below. The same stratified fluid was used for several experiments with the time between successive experiments kept to at least two hours to ensure that the linear stratification was re-established and that the internal wave field was totally damped. Shadowgraphs were also used to visualize the turbulent wake; see Lin et al. (1992a) for a detailed description of the technique.

3 Experimental results

As pointed out by Hopfinger et al. (1991) and Lin et al. (1992b), the nature of turbulent wakes of stratified flows past blunt obstacles varies with changes in the system parameters Re and Fi. For $Fi \lesssim 2.0$, the turbulent wake tends to contract vertically for a normalized streamwise distance $Nt = (X/D)\ Fi^{-1} \approx 1.5$, and then grows downstream to a maximum thickness of approximately the sphere diameter. When $Fi \gtrsim 2.0$, the wake grows vertically to a maximum thickness and then collapses downstream, again to a thickness of approximately the sphere diameter. One of the features that has not been studied in detail is the variation in the turbulent wake structure as a function of

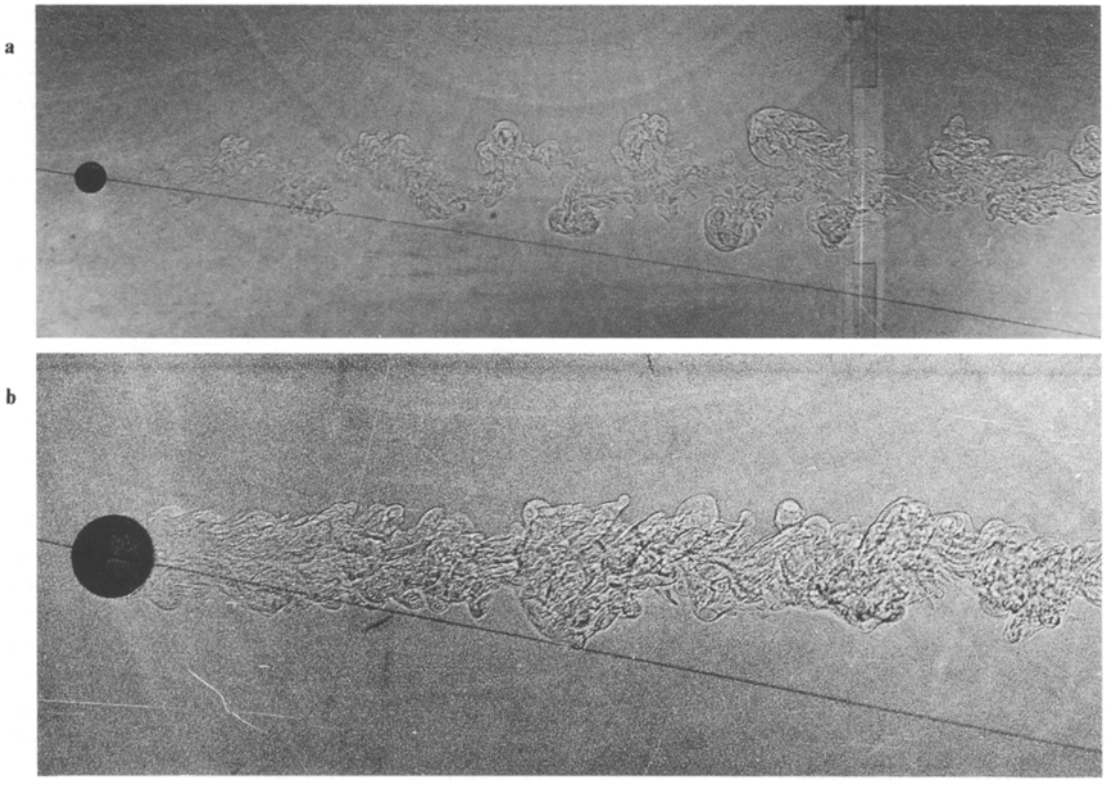

Fig. 2a and b. Side-view shadowgraphs for (**a**) large-scale coherent structures regime; $Re = 3580$, $Fi = 11.4$ and (**b**) the small-scale structures regime, $Re = 3{,}050$, $Fi = 3.0$

Re and *Fi*. Careful observations show that at relatively large *Re*, *Fi* combinations the turbulent wake tends to undulate (spiral) with respect to the streamwise centerline; the shadowgraph of Fig. 2a exemplifies this characteristic flow. Here stratification is not important in the near wake and large coherent structures which spiral around the streamwise axis are found in the lee of the sphere. The spiral structures have been observed in studies of sphere wakes in homogeneous fluids; e.g., Taneda (1978) and Sakamoto and Haniu (1990). The spiral structures were also observed to alternate sporadically in time. These spiral structures, owing to stratification, eventually collapse from $Nt \approx 2$ to 8. We define this characteristic wake as the "large-scale coherent structures" regime; this regime is shown by the symbol T_s in the flow regime diagram (*Fi*–*Re*) shown in Fig. 3. At smaller *Re*, *Fi* combinations, relative to the T_s regime, the turbulent wake viewed from either the side or the top is roughly symmetric across the streamwise centerline (i.e., there is no evidence of the occurrence of large-scale coherent structures); Fig. 2b exemplifies this regime. This characteristic flow is termed the "small-scale structures" regime and is designated by the symbol T on Fig. 3. The boundary between T (small-scale structures regime) and T_s on Fig. 3 must be considered as approximate since the transition between these characteristic motions is a gradual one.

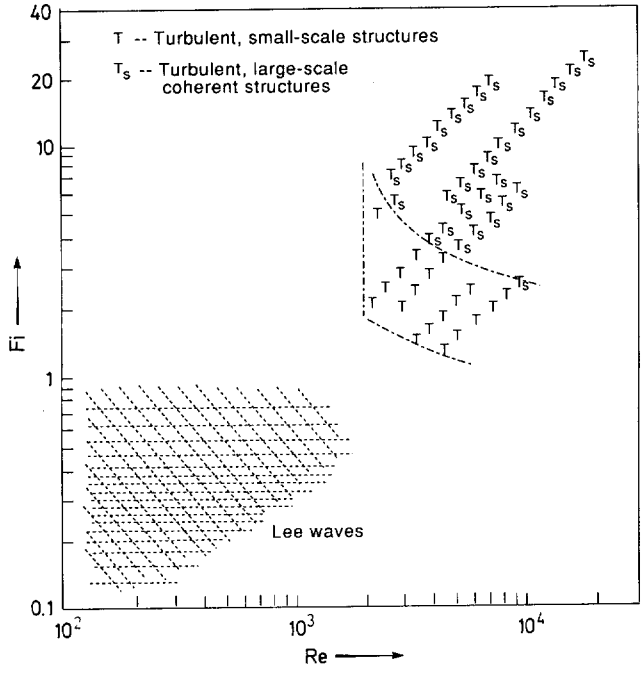

Fig. 3. Partial *Re* against *Fi* regime diagram expanded by T_s regime from Lin et al. (1992a) indicating the sphere generated lee wave regime and location of specific experimental runs in the large-scale spiralling coherent structures (T_s) and the small-scale structures (T) regimes

Note that the regime diagram of Fig. 3, although now differentiating between the T and T_s regimes (and including higher Re, Fi experiments) covers only a part of the Re, Fi diagram of the extensive study by Lin et al. (1992a); the general region for which obstacle generated lee waves dominate is indicated by the cross-hatched area in Fig. 3.

Observations of the large-scale coherent structures regime indicate that the spiralling structures grow downstream until $Nt \approx 2$, and then begin to collapse owing to stratification until $Nt \approx 8$. Because of the forcing induced by the generation and downstream propagation of the spiralling structures, large-amplitude internal waves having similar wave length as the streamwise length of the spiralling structures were indicated clearly on the particle streak photographs. An example of the generation and evolution of such waves is shown by the time sequence of particle streak photographs in Figs. 4a–c.

The photograph of Fig. 4a was taken during the time interval for which the sphere traversed a portion of the field of observation. The horizontal white streak on the right of the photograph designated by the arrows is due to light reflection from the center of the sphere; the line thus represents the sphere trajectory. Define the left-most position of the sphere trajectory of Fig. 4a as $Nt = 0$ (vertical arrow); using $Nt = Fi^{-1}(X/D)$ the right-side arrow then represents $Nt = 2$ (the exposure time is 2 s). The left and right sides of the photographs of Figs. 4b, c, respectively, represent the approximate Nt values given in the caption.

The vertical location of the sphere is indicated by the markings on the left side of each photograph, which is in

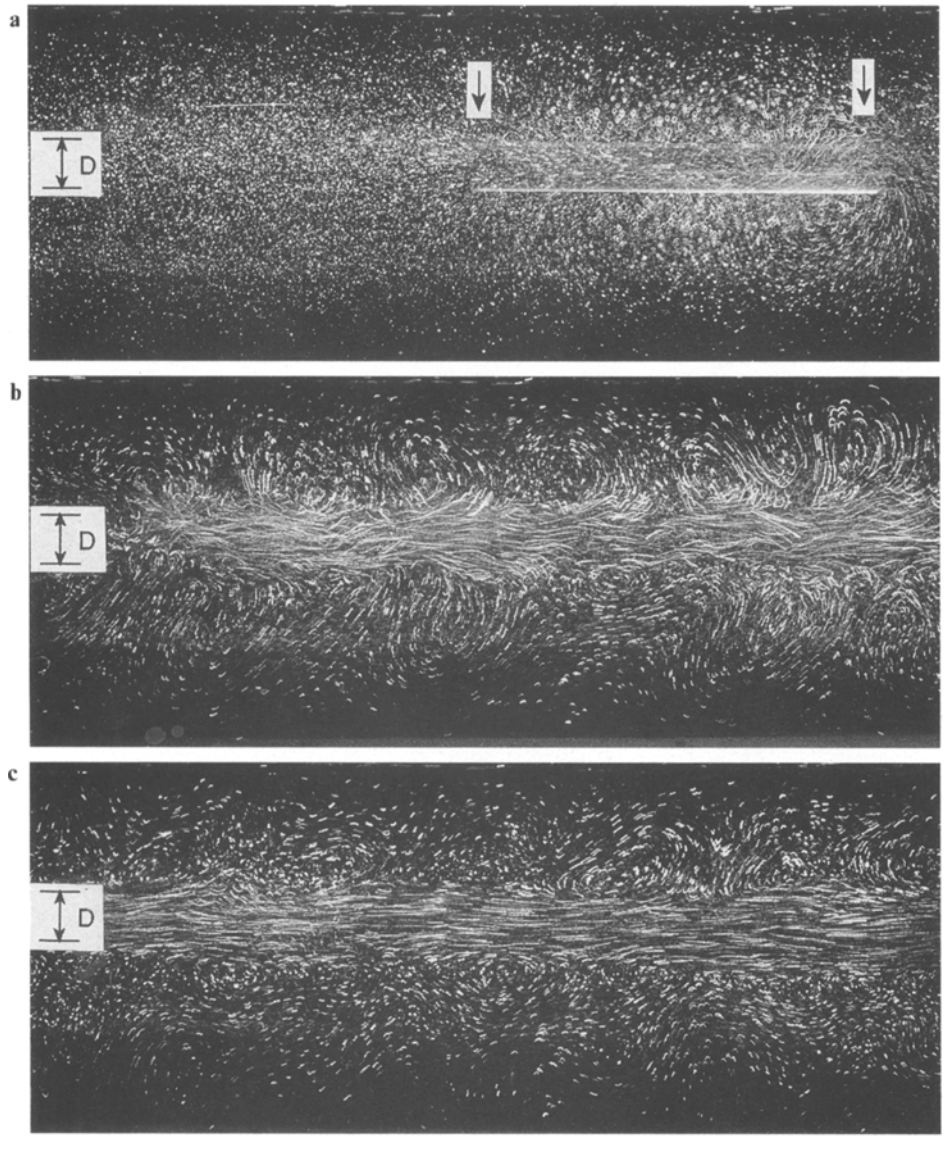

Fig. 4a–c. Particle streak photographs exemplifying the internal waves generated by a turbulent wake; $Re = 4{,}060$, $Fi = 4.60$, $D/H = 0.12$ and $T_e = 2$s (exposure time) for (**a**) and $T_e = 4$s for (**b**), (**c**). The camera is fixed with respect to the tow tank and the sphere is moving from right to left. The horizontal white line in (**a**) is due to a reflection from the sphere center and thus represents the sphere trajectory. The markings on the left of each photograph indicate the vertical position of the sphere. The left and right vertical arrows above (**a**) represent the dimensionless times $Nt = 0$, 2; the left and right sides of the photographs in (**b**) represent $Nt \approx 10$, 14 and in (**c**) 30, 34.

the approximate center of the tank. Metal horizontal supports along the top of the tank, however, block portions of the field of view with the result that the sphere location is somewhat above the horizontal centerline in the photographs.

Figure 4b, a photograph for $10 \lesssim Nt \lesssim 14$, shows clearly the internal wave field outside the turbulent wake. By this Nt, Lin et al. (1992b) have shown that the turbulent wake has collapsed to a thickness approximating the sphere diameter D. It is observed that in this example, the internal waves are not as uniformly distributed as those in Fig. 6a shown below. Fig. 4c is for $30 \lesssim Nt \lesssim 34$ and shows that the large amplitude waves have been damped somewhat compared to those of Fig. 4b. Internal waves were found to persist to $Nt \approx 100$, at which time their amplitudes had decreased below that of the scale resolvable from particle streak photographs. Waves at such large Nt are most likely reflections due to confinement effects since the "fossilized" turbulence may not generate waves.

Figures 5a–c represent a series of particle streak photographs for the internal wave field for different Re, Fi combinations. The designations for the sphere location and Nt values are given in the same fashion as for Figs. 4a–c. Fig. 5a shows the internal wave field in the range $15 \lesssim Nt \lesssim 17$ for a large Fi value. The internal wave field is depicted more clearly on the lower portion of the photograph due to the higher particle concentration in the lower part of the tank. The internal waves are well organized and the wave length and amplitude can readily be estimated. Note again that part of the upper portion of the flow field is blocked by the frame of the tank. Fig. 5b is a photograph for a relatively small Fi value in the large scale coherent

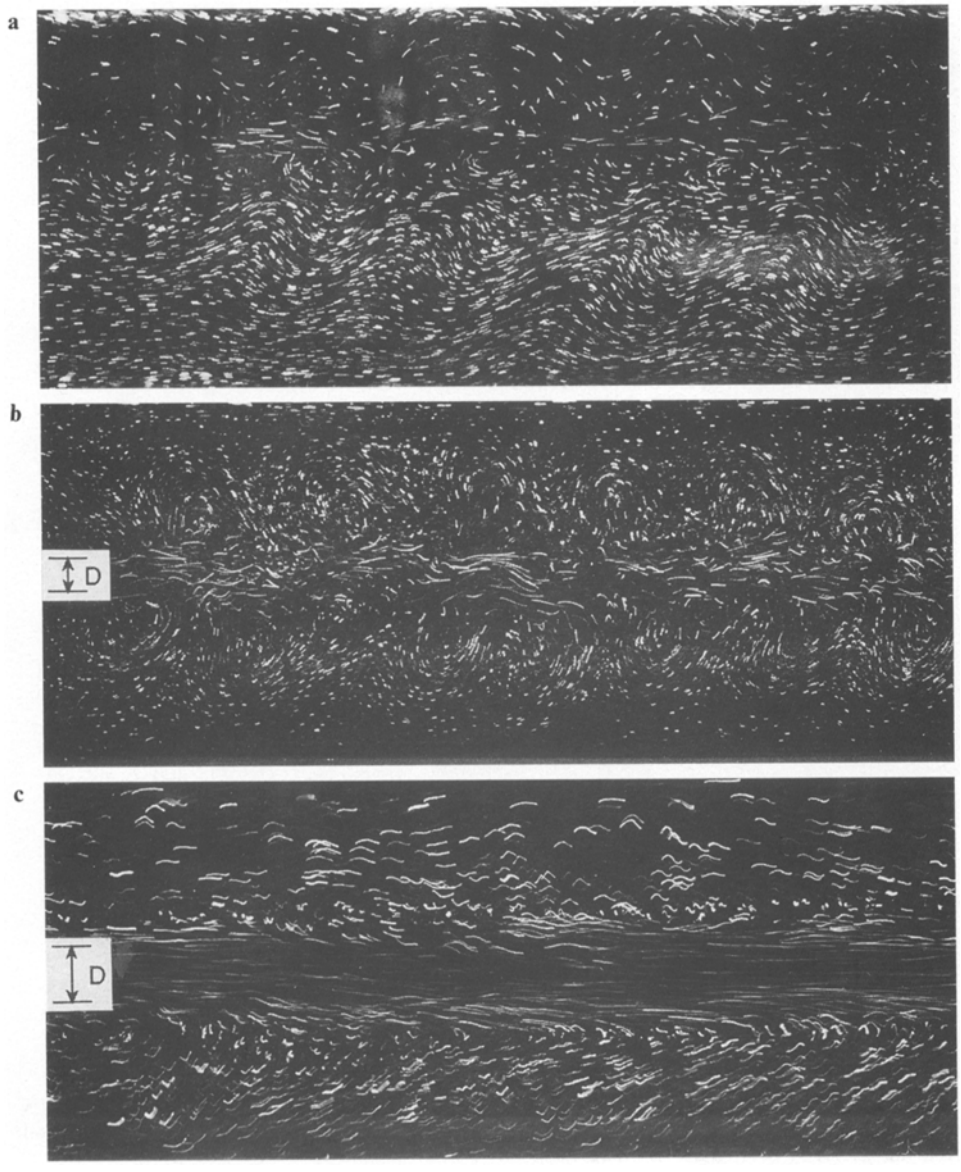

Fig. 5a–c. Particle streak photographs exemplifying the internal wave field for different Fi, Re combinations. **(a)** $Re = 7{,}050$, $Fi = 20.9$, $D/H = 0.07$, $15 \lesssim Nt \lesssim 17$, $T_e = 2$s; **(b)** $Re = 3{,}420$, $Fi = 10.76$, $D/H = 0.07$, $10 \lesssim Nt \lesssim 13$, $T_e = 3$s; **(c)** $Re = 7{,}300$, $Fi = 3.10$, $D/H = 0.21$, $12 \lesssim Nt \lesssim 18$, $T_e = 6$s

structures regime for the interval $10 \lesssim Nt \lesssim 12$. The internal wave field is again apparent outside of the collapsed wake. In this case, the waves are better organized compared with those in Fig. 4b. The maximum amplitude and the length of the resulting internal waves can be estimated from photographs such as Figs. 5a,b. At *Re*, *Fi* combinations within the small-scale structures regime, the undulating motions (coherent structures) are absent and hence the internal waves generated take the form of small amplitude, short random waves which persist for times as large as $Nt \approx 250$, as shown on Fig. 5c. Note that the exposure time is longer in Fig. 5c compared to those for Figs. 5a,b.

4 Quantitative observations

(*a*) *Length of dominant internal waves in T_s regime.* Particle streak photographs were used to measure the wave length of the dominant internal waves that are excited outside the wake region. The measurements were taken at $Nt \approx 10$, for different Froude numbers and at high *Re* to ensure the existence of large scale coherent structures. The normalized wave length λ/D so obtained is plotted against *Fi* in Fig. 6; the limited data of Hopfinger et al. (1991) are also included. The latter measurements were taken using dye tracers released from a rake of dye lines. In general, the present measurements are in agreement with those of Hopfinger et al. (1991). The present measurements further show an increase of the normalized wave length λ/D with *Fi* until $Fi \approx 10$, and levelling off thereafter to a value $\lambda/D \approx 5.5$. This conclusion assumes that the Reynolds numbers are sufficiently large for the turbulence to be Reynolds number independent.

(*b*) *Streamwise length of coherent structures.* Measurements of the streamwise length of the coherent structures (as defined in the insert of Fig. 7) were obtained from side view shadowgraphs of the wake; see, for example, Fig. 2a. Fig. 7 is a plot of the normalized length, c/D, of the spiral structures against *Fi*. Note that c/D initially increases with *Fi* and then levels off at a maximum value of $c/D \approx 5.5$. This value corresponds to a Strouhal number of 0.18, which is much the same as for vortex shedding of turbulent wakes of spheres in homogeneous fluids (Kim and Durbin 1988). The decreasing values of c/D with decreasing *Fi*, at smaller *Fi*, demonstrate the suppression of large coherent structures by stratification in more strongly stratified flows.

The variation of the ratio of the length of coherent structures to the mean length of the internal waves, c/λ_0, with *Fi* is given in Fig. 8; here the mean wavelength λ_0 of the internal waves as a function of *Fi* is obtained from the data of Fig. 6. These data show that the wave length of the internal waves is of the same order as the streamwise

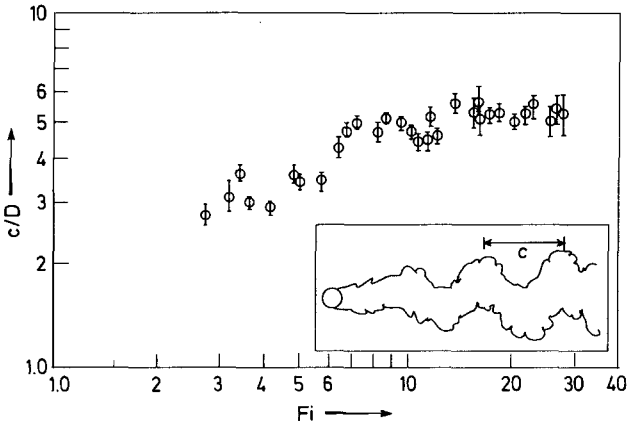

Fig. 7. Normalized streamwise length of coherent structures against Froude number *Fi*

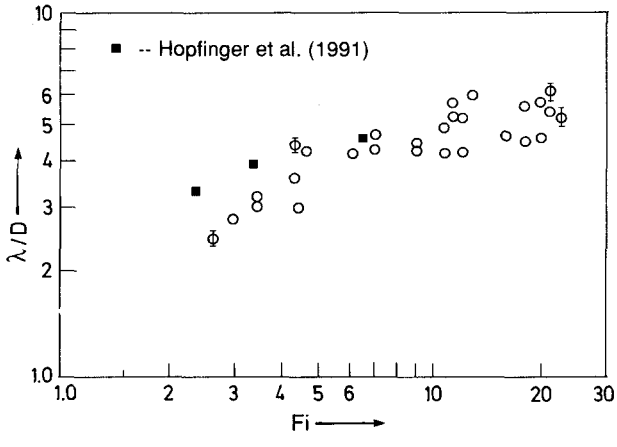

Fig. 6. Normalized length of the dominant wave λ/D against Froude number *Fi*. The wave length was measured at $Nt \approx 10$. Experiments from Hopfinger et al. (1991) are also included

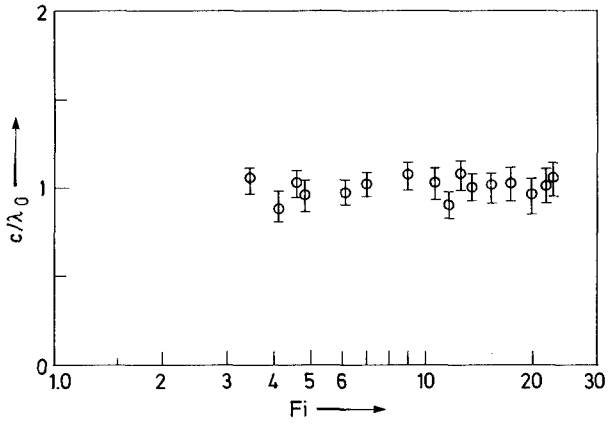

Fig. 8. Ratio of streamwise length of coherent structures to wavelength of dominant internal waves c/λ_0 against Froude number *Fi*

length of the coherent structures and is independent of Fi.

(*c*) *Temporal variation of wave length.* Figure 9 is a plot of the normalized dominant wave length against the normalized time Nt for several Re, Fi combinations. The measurements by Chomaz et al. (1990) are also incorporated (solid symbols). The present experiments show that the normalized wave length λ/D is roughly a constant, given by $\lambda/D \approx 5$. Chomaz et al. (1990) observed that the wave length increases with Nt at early times and then drops to a value $\lambda/D \approx 4$. Although such behavior might be expected for the wave amplitude, it is difficult to explain this latter trend for the wavelength on physical grounds.

(*d*) *Wave amplitude.* The normalized maximum amplitude, γ_m/D of waves was measured from photographs for the large-scale coherent structures regime and the results are shown in Fig. 10. The measurements were taken for $Nt \approx 5$ and 10 near the collapsed wake, where the maximum was likely to occur. The dashed line represents the mean value of the maximum heights of the turbulent wake obtained from shadowgraphs by Lin et al. (1992b). It is observed that the maximum wave amplitude increases with Fi in a manner similar to that for the maximum turbulent wake height. The internal wave amplitudes, however, were smaller than the maximum turbulent wake heights. It is concluded that the dominant mode of internal waves is induced by the large spiralling motions of the turbulent wake. On physical grounds, one should expect that the maximum wave height be equal or less than the maximum thickness of the wake.

(*e*) *Frequency of the dominant waves.* The frequency of the dominant waves was detected by placing a conductivity probe in the far downstream ($Nt \approx 5.0$ and 10) but outside the wake. The period of the energy containing waves was estimated to be about 15–20 s from the time record of the density fluctuations. Due to the length limit of the tow tank, the experiments were of too short a duration to accurately measure the period of the dominant waves from the power spectrum of the density fluctuations.

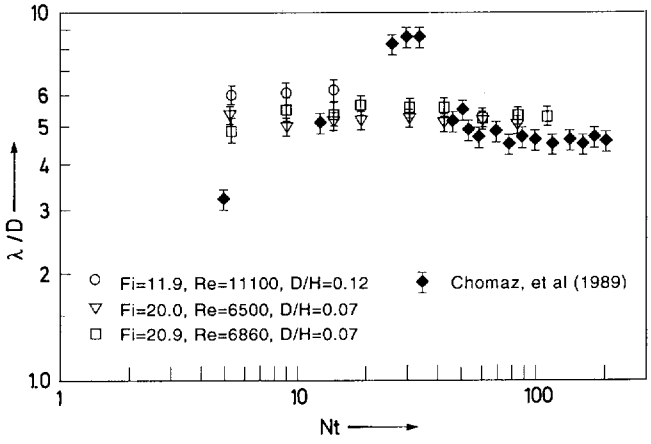

Fig. 9. Dimensionless temporal variation of the normalized wavelength of the dominant internal waves λ/D for various Fi, Re and D/H. Experiments from Chomaz et al. (1989) are also included

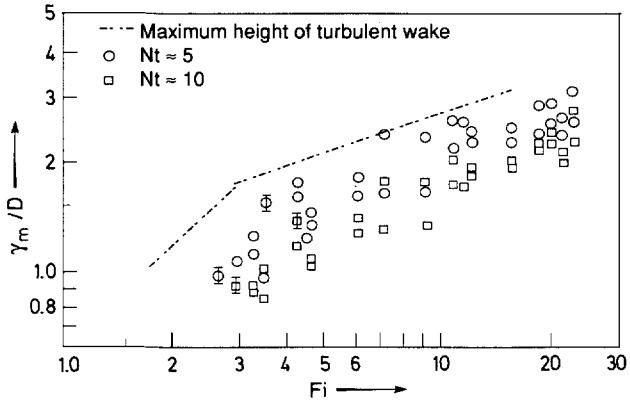

Fig. 10. Normalized maximum internal wave amplitude γ_m/D against Froude number at $Nt \approx 5$ and 10; note that the maximum amplitude is bounded from above by the maximum height of the turbulent wake as obtained from shadowgraphs

5 Conclusions

Some properties of internal waves generated by the turbulent wake behind a sphere moving horizontally through a linearly stratified fluid were studied using flow visualization techniques. The Reynolds and internal Froude number ranges investigated were: $2{,}000 \leq Re \leq 12{,}900$ and $2.0 \leq 28.0$, respectively. Two characteristic turbulent wake regimes were identified. The first is the large-scale coherent structures regime at relatively large Re, Fi combinations and the second, a small-scale structures regime, at smaller Re, Fi values.

The study demonstrated that the dominant internal waves are generated by the large-scale coherent structures in the T_s regime, and that the wavelengths of these waves scale with the streamwise length of the coherent structures. Furthermore, the maximum amplitude of the internal waves was measured and shown to be bounded from above by the maximum height of the turbulent wake which is known to be a function of Fi. In the "small scale structures" regime, the internal wave fields for the most part consisted of short, small amplitude waves.

Acknowledgements

The authors acknowledge, with thanks, the support of the Office of Naval Research under its Accelerated Research Initiative on Vortex Dynamics, Grant No. N00014-90-J-4063, and the National Science Foundation.

References

Brighton, P. W. M. 1978: Strongly stratified flow past three-dimensional obstacles. Q. J. Roy. Met. Soc. 104, 289–307

Castro, I. P.; Snyder, W. H.; Marsh, G. L. 1983: Stratified flow over three-dimensional ridges. J. Fluid Mech. 135, 261–282

Chomaz, J. M.; Bonneton, P.; Butet, A.; Hopfinger, E. J.; Perrier, M. 1990: Gravity wave patterns in the wake of a sphere in a stratified fluid. Proceedings of Turbulence 89, (Eds. Lesieur, M.; Metais, O.). Kluwer Academic Publishers, Dordrecht, The Netherlands

Crapper, G. D. 1959: A three-dimensional solution for waves in the lee of mountains. J. Fluid Mech. 6, 51–76

Gilreath, H. E.; Brandt, A. 1985: Experiments on the generation of internal waves in a stratified fluid. AIAA J. 23, 693–700

Hanazaki, H. 1988: A numerical study of three-dimensional stratified flow past spheres. J. Fluid Mech. 192, 303–419

Hopfinger, E. J.; Flor, J. B.; Chomaz, J. M.; Bonneton, P. 1991: Internal waves generated by a moving sphere and its wake in a stratified fluid. Exp. Fluids 11, 255–261

Kim, H. J.; Durbin, P. A. 1988: Observations of the frequency in a sphere wake and of drag increase by acoustic excitation. Phys. Fluids 31, 3260–3265

Lighthill, M. J. 1978: *Waves in fluids*. London: Cambridge University Press

Lin, Q.; Boyer, D. L.; Fernando, H. J. S. 1992a: Stratified flow past a sphere. J. Fluid Mech. 240, 315–355

Lin, Q.; Boyer, D. L.; Fernando, H. J. S. 1992b: Turbulent wakes of linearly stratified flow past a sphere. Phys. Fluids (A) 4 (8), 1687–1696

Mowbray, D. E.; Rarity, B. S. 1967: A theoretical and experimental investigation of the phase configuration of internal waves of small amplitude in a density stratified liquid. J. Fluid Mech. 28, 1–16

Sakamoto, H.; Haniu, H. 1990: A study on vortex shedding from spheres in a uniform flow. J. Fluids Eng. (Trans. ASME) 112, 386–392

Schooley, A. H.; Hughes, B. A. 1972: An experimental and theoretical study of internal waves generated by the collapse of a two-dimensional mixed region in a density gradient. J. Fluid Mech. 51, 159–175

Taneda, S. 1978: Visual observations of the flow past a sphere at Reynolds numbers between 10^4 and 10^6. J. Fluid Mech. 85, 187–192

Wu, J. 1969: Mixed region collapse with internal wave generation in a density stratified medium. J. Fluid Mech. 35, 531–544